

# Direct Detection of Nucleic Acids by Tagging Phosphates on Their Backbones with Conductive Nanoparticles

Yi Fan, Xiantong Chen, Jinming Kong, Chih-hang Tung, and Zhiqiang Gao\*

Over the past decade, many technological advances have been made in the use of nanotechnology for biosensing.<sup>[1–3]</sup> Coupled with the development of optical, electrochemical, electrical, and other techniques for monitoring biorecognition events on solid devices and in solution, intensive research efforts have been put into realizing accurate, sensitive, selective, and portable biosensors for both laboratory and point-of-care applications. Nanoparticles, in particular, have been studied extensively in biosensors for nucleic acids and proteins.<sup>[2,3]</sup> These particles are unique because their nanometer size gives rise to a high reactivity and beneficial physiochemical properties that are chemically tailorable. Utilization of nanoparticles has translated into new assays that improve on current methods of nucleic acid and protein detection.

In a milestone discovery in 1996, Mirkin et al. reported unique optical and melting properties of an aggregate of Au nanoparticles and oligonucleotides.<sup>[4]</sup> Nanoparticle probes have since been demonstrated to be advantageous over conventional probes in many detection schemes.<sup>[3,4]</sup> Among them, direct electrical detection is one of the simplest and most sensitive methods.<sup>[3]</sup> In the electrical detection scheme, capture probes are immobilized in micron-sized gaps between electrodes in an array. Hybridization with target nucleic acids and detection probes tagged with Au nanoparticles localizes the nanoparticles in the gaps, whereas subsequent Ag deposition (amplification) creates “bridges” across the gaps. The detection of a conductance change results in a detection limit of 500 fM.<sup>[3]</sup> Unfortunately, the current amplification strategies for electrical signal generation often involve multiple steps of deposition or enhancement. Hence, there is a trade off between simplicity and sensitivity. Nonetheless, the eventual acceptance of nanoparticle-based electrical biosensors for diagnostic applications will depend on how these novel systems compare with the current gold standards, that is, polymerase chain reaction and enzyme-linked immunosorbent assay, in terms of simplicity, sensitivity, specificity, portability, and reliability.

Tremendous opportunities exist in the application of nanoparticles for biosensors. Indium tin oxide (ITO) nanoparticles, which are electrically conductive, have therefore been exploited herein for possible applications in electrical nucleic acid biosensors. The association of these nanoparticles with hybridized nucleic acid molecules leads to the formation of an ITO nanoparticle network in the gaps that significantly increases the conductance, directly signaling the presence of target nucleic acids in the sample solution without amplification or Ag enhancement.

Figure 1 shows the working principle of the biosensor. A monolayer of peptide nucleic acid (PNA) capture probes was

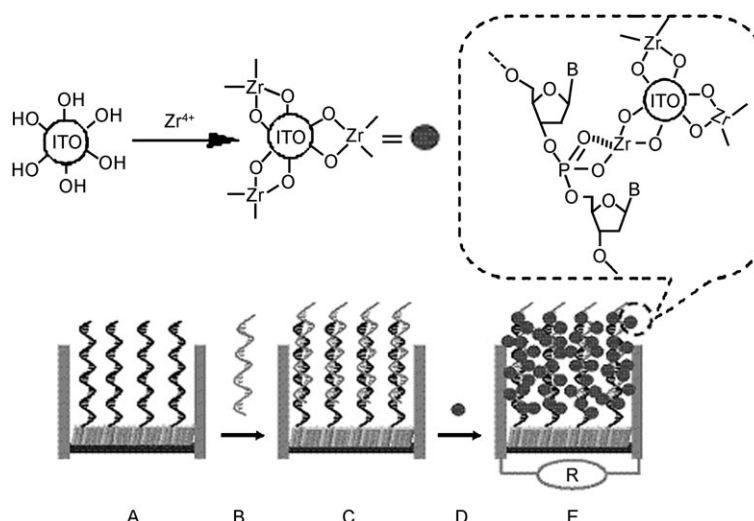


**Figure 1.** Schematic representation of the nucleic acid biosensor based on direct tagging of the hybridized target nucleic acid with ITO nanoparticles and electrical detection.

assembled in the nanogaps ( $\approx 300$  nm) of a pair of interdigitated electrodes through silane chemistry, which then acts as a biosensing interface (A). The interaction of PNA with sample nucleic acid (B) forms a heteroduplex, bringing a high density of phosphates to the biosensor surface (C). The phosphates of the hybridized nucleic acids serve as anchoring sites, providing the requisite local environment to facilitate direct tagging, and the ITO nanoparticles are the tags. As a result, the hybridized nucleic acid molecules are tagged with multiple ITO nanoparticles (D). The formation of the electrical conductive ITO nanoparticle network in the gaps provides much needed sensitivity for the detection of nucleic acids (E). To minimize non-hybridization-related uptake of ITO and to increase the hybridization efficiency, the neutral

[\*] Dr. Y. Fan, Dr. X. Chen, Dr. J. Kong, C.-h. Tung, Dr. Z. Gao  
Institute of Microelectronics  
11 Science Park Road  
Singapore 117685 (Singapore)  
Fax: (+65) 6773-1914  
E-mail: gaozq@ime.a-star.edu.sg

and phosphate-free character of the PNA capture probes alleviates the interaction between surface-immobilized capture probes (for example, oligonucleotides) and the cationic ITO nanoparticles and the electrostatic repulsion of duplex formation,<sup>[5,6]</sup> producing a high signal/noise ratio. Furthermore, the mismatch discrimination of PNA is in many cases much better than that of DNA, offering a much higher specificity.<sup>[7]</sup>

First, the feasibility of utilizing the ITO nanoparticles as novel tags for possible applications in nucleic acid biosensors was evaluated. Figure 2 compares the conductance changes of

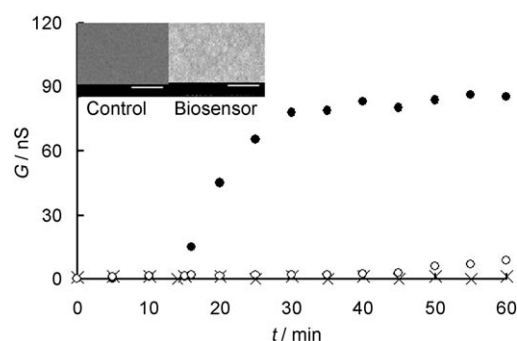


**Figure 2.** The dependence of conductance of 100 pM complementary (●), one-base-mismatched (○), and control sample (x) oligonucleotides on incubation time in  $10 \mu\text{g mL}^{-1}$  ITO nanoparticles in pH 4.0 buffer solution with 0.10 M  $\text{NaNO}_3$ . Hybridization for 60 min in pH 8.5 buffer solution with 10 mM Tris-HCl, 1.0 mM EDTA, and 0.10 M NaCl buffer solution at  $50^\circ\text{C}$ . Insets: SEM images of the corresponding biosensor and the control biosensor, respectively; scale bar: 100 nm.

the biosensors after various treatments. Upon hybridization, complementary target nucleic acid molecules were selectively captured and bound to the biosensor with the ITO nanoparticles in which little if any of non-complementary (control) nucleic acid was captured during hybridization. As expected, minute conductance changes were observed at the biosensor after hybridization to the control nucleic acid and incubation with the ITO nanoparticles. As shown in Figure 2, after hybridization with the complementary target nucleic acid and incubation with the ITO nanoparticles, a substantial increase in conductance, by as much as 100-fold, was observed, which paves the way for ultrasensitive detection of nucleic acids. Extensive washing with acidified 0.10 M  $\text{NaNO}_3$  solution removed most of the non-hybridization-related ITO nanoparticle uptake. These results clearly demonstrated that the target nucleic acid is successfully tagged by the ITO nanoparticles and that the ITO nanoparticles form conductive paths, effectively bridging the insulating gaps. Phosphates and phosphonates are known to interact strongly with transition-metal oxides such as titanium oxide, niobium oxide, and zirconium oxide in particular to form relatively stable interfacial bonds.<sup>[8–15]</sup> The zirconium/zirconia phosph(on)ate chemistry was first pioneered by Mallouk to construct ordered organic thin films.<sup>[14,15]</sup> Furthermore, strong interaction between ITO and phosphate is also observed.<sup>[16,17]</sup> The demonstration that zirconium and zirconia initiated phosphate monolayer and multilayer formation under ambient

conditions suggests that the significant increase in conductance is indeed a consequence of the formation of conductive nanoparticle paths in the gaps through direct tagging of the phosphate backbone with the ITO nanoparticles. The enhancement in conductance is directly proportional to the concentration of nucleic acid in the sample solution. The combination of highly efficient PNA/DNA hybridization, direct multiple ITO nanoparticle tagging, and electrical detection provides a generic platform with a greatly simplified procedure for nucleic acid quantification.

Next, the specificity of the biosensor was evaluated by analyzing fully complementary, one- and two-base mismatched oligonucleotides. It was found that the ITO nanoparticle tagging procedure offers excellent discrimination against mismatched sequences. As seen in Figure 2, a conductance increment for the biosensor hybridized to the complementary target was in the range of 75–86 nS. If it was replaced by mismatched targets ( $\text{A} \leftrightarrow \text{T}$  or  $\text{G} \leftrightarrow \text{C}$  mismatch in the middle of target nucleic acids), the conductance increment dropped by as much as 95% when one base was mismatched and it was indistinguishable from the background when two bases were mismatched. The good mismatch discrimination probably originates from the use of PNA as capture probes and the direct multiple tagging. As mentioned earlier, PNA capture probes often offer better mismatch discrimination.<sup>[7]</sup> The ITO nanoparticle tagging procedure may also contribute significantly to the specificity of the biosensor. To have a measurable conductance change, the ITO nanoparticle tags must reach a critical mass, sufficient to bridge up the electrode gaps. Below the critical mass, the conductance is indistinguishable from that of the background. Even better specificity would be expected at lower concentrations. Indeed, practically no conductance changes were observed for both the one- and two-base mismatched sequences at concentrations below 25 pM.

Finally, the analytical characteristics of the biosensor were investigated. Three target nucleic acids with lengths ranging from 22 to 60 nucleotides (nt) were used. As illustrated in Figure 3, the dynamic ranges for the 22-, 40-, and 60-nt target nucleic acids were 0.10–100 pM, 0.050–50 pM, and 0.050–50 pM, with relative standard deviations of 15–22% and detection limits of 50 fM, 25 fM, and 25 fM, respectively.

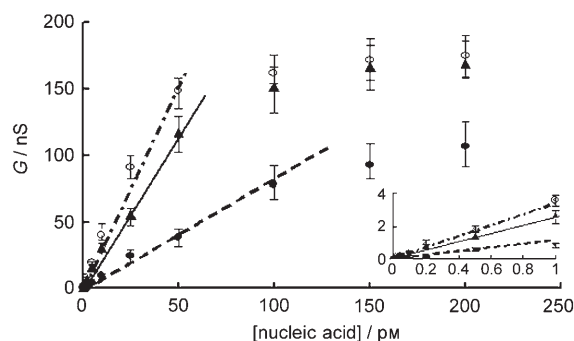


**Figure 3.** Calibration curves for 22- (●), 40- (▲), and 60-nt (○) target nucleic acids. Inset: calibration curves at low concentration values. Hybridization was performed for 60 min at  $50^\circ\text{C}$ , other conditions are as for Figure 2.

Compared with previous nanoparticle-based nucleic acid biosensors, the sensitivity was greatly improved by adopting the ITO nanoparticle tagging procedure. In the biosensors reported earlier, the ratio of the nanoparticle tag and target nucleic acid molecule was fixed at 1:1. The amount of capture probes immobilized on the biosensor surface and hybridization efficiency determine the amount of target nucleic acid bound to the surface and thereby the amount of nanoparticle tags. It was practically impossible to detect traces of nucleic acid without the amplification step.<sup>[3,4]</sup> However, in our procedure, multiple ITO nanoparticle tags on a single nucleic acid strand increase the tag loading, greatly enhancing the response of the electrical detection and hence the sensitivity and detection limit of the biosensor. The sensitivity is now determined by the density of the ITO nanoparticles, which in turn was determined by the total number of phosphates in the gaps. Hypothetically, if ITO tagging and hybridization efficiency remain unchanged for all target nucleic acids, the same current sensitivity per base should be obtained. At the same molar concentration, the sensitivity should be roughly proportional to the length of the target nucleic acid. Although it was found that the sensitivity is dependent on the length of the target nucleic acid—the longer the nucleic acid, the higher the sensitivity (Figure 3)—no straightforward relationship between the length and sensitivity was observed. This suggests that the tagging and hybridization efficiency are also dependent on the length of the target nucleic acid. The use of the ITO nanoparticles has two major benefits over other nanoparticle approaches. One is direct tagging, which alleviates the use of the second oligonucleotide detection probes. Direct tagging is thus particularly relevant for extremely short target nucleic acids, such as microRNA (miRNA) molecules. The other is the simplicity of the procedure, which offers great opportunity for further development of the biosensor into a practical system.

In conclusion, the biosensor described herein is rapid, ultrasensitive, and is able to directly detect nucleic acids without involving biological ligation or detection probes. By employing ITO nanoparticles, nucleic acids were directly tagged with multiple electrically conductive ITO nanoparticles under very mild conditions. Specific nucleic acids were detected electrically at femtomolar levels by simply measuring the conductance changes with high specificity. It is particularly attractive to the development of message RNA and miRNA expression profiling tools.

### Experimental Section

The ITO nanoparticles, butylamine, and sodium borohydride (>99%) were purchased from Sigma-Aldrich (St Louis, MO). Trimethyloxysilane aldehyde (90%) was purchased from United Chemical Technologies Inc. (Bristol, PA). Amino-terminated PNA capture probes (N→C: NH<sub>2</sub>-AAC CAC ACA ACC TAC TAC CTC A) used in this work were custom made by Eurogentec (Herstal, Belgium) and all other oligonucleotides of PCR purity were from 1st Base Pte Ltd. (Singapore). The sequences of oligonucleotides used in this work are as follows: 5'-TGA GGT AGT AGG TTG TGT GGT T-3' (target 1, 22 nt), 5'-TGA GGT AGT AGG TTG TGT GGT TAT GTC TAA GGC ATT ACA C-3' (target 2, 40 nt), 5'-TGA GGT AGT AGG TTG TGT GGT TAT GTC TAA GGC ATT ACA CAA ATC

AAA GAT CTA CAT GGA-3' (target 3, 60 nt), 5'-TGA GGT AGT AGG ATG TGT GGT T-3' (one-base mismatched, 22 nt), 5'-TGA GCT AGT AGG TTG TGA GGT T-3' (two-base mismatched, 22 nt), and 5'-CAA AAC AAA GAT CTA CAT GGA T-3' (control, 22 nt). All other reagents of certified analytical grade were obtained from Sigma-Aldrich and used without further purification. A pH 8.5 buffer solution of 10 mM Tris-HCl, 1.0 mM EDTA, and 0.10M NaCl was used as the hybridization and washing buffer solution. A pH 4.0 buffer solution of 0.10M NaNO<sub>3</sub> was used as the incubation medium for direct ITO nanoparticle tagging.

Electrical measurements were performed with an Advantest R8340 A ultrahigh resistance meter (Advantest Corp., Tokyo, Japan). The biosensor consists of a pair of interlocking comblike structures (electrodes) with 150–200 fingers, each 700-nm wide and 200-μm long, and with a 300-nm gap between the fingers of the two electrodes.

The ITO nanoparticles were first activated by ZrOCl<sub>2</sub> to produce stable Zr<sup>4+</sup> anchoring sites for phosphates on the ITO nanoparticle surface (Figure 1). The stable attachment of Zr<sup>4+</sup> onto the ITO nanoparticles is believed to originate from an ion-exchange reaction of a hydroxide on the ITO nanoparticle surface and ZrOCl<sub>2</sub>.<sup>[9]</sup> ZrOCl<sub>2</sub> (50 mg) and water (0.20 mL), were added to ITO (0.50 g), and the resulting slurry was mechanically grinded for 120–150 min. The mixture was suspended in ethanol (10 mL) and was centrifuged at 12000 rpm for 20 min. The ITO nanoparticles were then suspended in alkalized ethanol (10 mL) and were centrifuged at 12000 rpm for another 20 min. They were then washed and centrifuged with ethanol several times. TEM experiments showed that the ITO nanoparticles are approximately cubic with a mean diameter of approximately 21 nm and comprised of In (61%), Sn (4%), O (34%), and Zr (≈0.05%).

The silanization of the biosensor was performed according to the method of Lieber and co-workers.<sup>[18]</sup> The immobilization of PNA capture probes was carried out as follows: amine-terminated PNA capture probes were denatured for 10 min at 90°C and diluted to a concentration of 5.0 μM in 0.10M acetate buffer solution at pH 6.0. An aliquot (25 μL) of the capture probes solution was dispensed onto the silanized biosensor and incubated for 2–3 h at 20°C in an environmental chamber. After incubation, it was rinsed successively with 0.10% SDS and water. The unreacted aldehyde moieties were blocked by butylamine in a 1.0 mM butylamine solution in the acetate buffer solution. The reduction of the imines was carried out by a 5-min incubation of the electrode in a 2.5 mg mL<sup>-1</sup> sodium borohydride solution made of PBS/ethanol (PBS = phosphate-buffered saline) (3:1). The biosensor was then soaked in vigorously stirred hot water (90–95°C) for 2 min and blown dry with a stream of nitrogen. The hybridization of the target nucleic acid and its electrical detection were carried out as illustrated in Figure 1. First, the biosensor was placed in an environmental chamber maintained at 50°C. A 25-μL aliquot of hybridization solution containing the target nucleic acid was uniformly spread onto the biosensor. After 60 min of hybridization, it was then rinsed thoroughly with a blank hybridization solution at 50°C. The ITO nanoparticles were tagged onto the phosphates of the hybridized target nucleic acids through zirconium phosphate chemistry after incubation for 30 min at 25°C with a 25-μL aliquot of 5–10 μg mL<sup>-1</sup> ITO nanoparticles in the pH 4.0 solution with 10M NaNO<sub>3</sub>. It was then thoroughly rinsed with the pH 4.0 solution with 0.10M NaNO<sub>3</sub> solution. Electrical measurements were carried out after the biosensor was completely dried in a nitrogen stream.

Received: September 4, 2006

Revised: December 15, 2006

Published online: February 9, 2007

**Keywords:** biosensors · indium tin oxide · nanotechnology · nucleic acids · zirconium

- [1] P. Fortina, L. J. Kricka, S. Surrey, P. Grodzinski, *Trends Biotechnol.* **2005**, 23, 168–173.
- [2] N. C. Tansil, Z. Gao, *Nano Today* **2006**, 1, 28–37.
- [3] N. L. Rosi, C. A. Mirkin, *Chem. Rev.* **2005**, 105, 1547–1562.
- [4] a) C. A. Mirkin, R. L. Letsinger, R. C. Mucic, J. J. Storhoff, *Nature* **1996**, 382, 607–609; b) S. I. Stoeva, J.-S. Lee, C. S. Thaxton, C. A. Mirkin, *Angew. Chem.* **2006**, 118, 3381–3384; *Angew. Chem. Int. Ed.* **2006**, 45, 3303–3306; c) J.-M. Nam, C. S. Thaxton, C. A. Mirkin, *Science* **2003**, 301, 1884–1886; d) D. G. Georganopoulou, L. Chang, J.-M. Nam, C. S. Thaxton, E. J. Mufson, W. L. Klein, C. A. Mirkin, *Proc. Natl. Acad. Sci. USA* **2005**, 102, 2273–2276; e) J.-M. Nam, S. I. Stoeva, C. A. Mirkin, *J. Am. Chem. Soc.* **2004**, 126, 5932–5933.
- [5] M. Egholm, O. Buchardt, L. Christensen, C. Behrens, S. M. Freier, D. A. Driver, R. H. Berg, S. K. Kim, B. Norden, P. E. Nielsen, *Nature* **1993**, 365, 566–568.
- [6] U. Giesen, W. Kleider, C. Berding, A. Geiger, H. Orum, P. E. Nielsen, *Nucleic Acids Res.* **1998**, 26, 5004–5006.
- [7] T. Ratilainen, A. Holmen, E. Tuite, P. E. Nielsen, B. Norden, *Biochemistry* **2000**, 39, 7781–7791.
- [8] W. Gao, L. Dickinson, C. Grozinger, F. G. Morin, L. Reven, *Langmuir* **1996**, 12, 6429–6435.
- [9] H. G. Hong, Y. Kim, *Electrochim. Acta* **2001**, 46, 2313–2319.
- [10] D. Brovelli, G. Hahner, L. Ruiz, R. Hofer, G. Kraus, A. Waldner, J. Schlosser, P. Oroszlan, M. Ehrat, N. D. Spencer, *Langmuir* **1999**, 15, 4324–4327.
- [11] J. P. Folkers, C. B. Gorman, P. E. Laibinis, S. Buchholz, G. M. Whitesides, R. G. Nuzzo, *Langmuir* **1995**, 11, 813–824.
- [12] M. Textor, L. Ruiz, R. Hofer, A. Rossi, K. Feldman, G. Hahner, N. D. Spencer, *Langmuir* **2000**, 16, 3257–3271.
- [13] F. Bellezza, A. Cipiciani, M. A. Quotadamo, *Langmuir* **2005**, 21, 11099–11104.
- [14] H. Lee, L. J. Kepley, H. G. Hong, T. E. Mallouk, *J. Am. Chem. Soc.* **1988**, 110, 618–620.
- [15] H. Lee, L. J. Kepley, H. G. Hong, S. Akhter, T. E. Mallouk, *J. Phys. Chem.* **1988**, 92, 2597–2601.
- [16] P. M. Armistead, H. H. Thorp, *Anal. Chem.* **2000**, 72, 3764–3770.
- [17] N. D. Popovich, B. K. Yen, S. S. Wong, *Langmuir* **2003**, 19, 1324–1329.
- [18] G. F. Zheng, F. Patolsky, Y. Cui, W. U. Wang, C. M. Lieber, *Nat. Biotechnol.* **2005**, 23, 1294–1301.